Indian Journal of Pure & Applied Physics
Vol. 64, October 2026, pp. 1083-1091
DOI: 10.56042/ijpap.v64i10.26746

Integrated Environmental Hazard and Human Health Risk Evaluation of Water Resources in the Okaba Coal Mining Region

Aruwa Arome[a,b*] & Walia Genius[a]

[a]Department of Physics, Guru Kashi University, Talwandi Sabo, Punjab 151 302, India

[b]Department of Physics with Electronics, Federal Polytechnic, Idah 271 101, Nigeria

Received: 19th December 2025; accepted: 27th August 2026

This study evaluated radiological contamination in water sources near the Okaba coal mining area, Ankpa, Kogi State, Nigeria. Twenty-four water samples were collected from streams, rivers, and boreholes adjacent to mining operations during October–December 2024. Activity concentrations of naturally occurring radionuclides (^{238}U, ^{232}Th, and ^{40}K) were determined using high-purity germanium (HPGe) gamma spectrometry. Measured ^{238}U activities ranged from 44.24 ± 0.33 to 172.67 ± 2.39 Bq L^{-1} (mean: 104.80 Bq L^{-1}), ^{232}Th from 21.66 ± 0.03 to 99.20 ± 0.91 Bq L^{-1} (mean: 51.49 Bq L^{-1}), and ^{40}K from 101.72 ± 0.18 to 987.24 ± 4.32 Bq L^{-1} (mean: 719.64 Bq L^{-1}). The mean radium equivalent activity (573.87 Bq L^{-1}) exceeded recommended limits. Average outdoor and indoor absorbed dose rates (109.53 and 210.63 nGy h^{-1}) surpassed global reference values by factors of 1.86 and 2.51. Estimated annual effective ingestion doses for infants, children, and adults (means: 6.88, 4.59, and 3.15 mSv y^{-1}) substantially exceeded WHO guidelines. Excess lifetime cancer risk values ranged from 12.57 × 10^{-3} (adults) to 27.45 × 10^{-3} (infants), markedly above benchmarks. These results demonstrate that coal mining activities have significantly enhanced natural radioactivity in local water resources, necessitating immediate regulatory intervention.

Keywords: Radiological hazard assessment, Naturally occurring radionuclides, Drinking water quality, Environmental radioactivity monitoring, Okaba coalfield

1 Introduction

Coal extraction constitutes a vital economic enterprise across numerous Nigerian states; however, these operations simultaneously generate substantial environmental and public health challenges through the mobilization of naturally occurring radioactive materials (NORMs). Within the Okaba coalfields situated in Ankpa, Kogi State, coal processing activities disturb the natural geochemical equilibrium, facilitating the release of radionuclides from geological formations into surrounding environmental compartments[1]. Among these compartments, aquatic systems represent the principal pathways for radionuclide dispersion, bioaccumulation, and subsequent human exposure. Communities adjacent to mining zones depend heavily on these water resources for drinking, domestic purposes, crop irrigation, and livestock watering.

The radionuclides warranting primary attention encompass uranium-238 (^{238}U) and thorium-232 (^{232}Th) decay chain components, particularly radium-226 (^{226}Ra), along with naturally abundant potassium-40 (^{40}K). These elements enter water systems through natural mechanisms including bedrock weathering and leaching, as well as anthropogenically accelerated processes such as overburden removal, coal beneficiation, mine pit drainage, and tailings disposal[2]. Epidemiological evidence demonstrates that sustained consumption of water containing elevated radionuclide concentrations correlates with increased cancer incidence, renal impairment, and developmental abnormalities[3,4]. Consequently, systematic radiological assessment of water resources proximate to mining operations constitutes an essential public health protection measure.

The Okaba coalfields, located within the mineral-rich Anambra Basin, represent significant contributors to Nigeria's energy and industrial coal production. Extensive mining activities have caused well-documented environmental deterioration, including widespread deforestation, accelerated erosion, and contamination of both surface and groundwater resources[5]. The region's hydrological dynamics facilitate the transport of particulate and dissolved radionuclides from mining sites to adjacent water systems, posing persistent threats to human populations and aquatic biodiversity.

*Corresponding author: E-mail: aroaruwa@gmail.com

Examination of existing Nigerian literature reveals research emphasis directed toward radiological hazards in alternative extractive sectors, including granite quarrying operations[6] and terrestrial gamma radiation assessments[7]. Although these investigations provide valuable insights, a notable deficiency exists regarding comprehensive, targeted research specifically examining water quality in coal mining regions. International studies conducted in analogous coal mining contexts consistently document radionuclide concentrations exceeding WHO drinking water quality guidelines[3,8,9]. The absence of localized baseline data for the Okaba region impedes effective risk communication, regulatory oversight, and mitigation strategy development. Accordingly, this investigation was undertaken to address this critical knowledge gap.

2 Materials and Methods

2.1 Study Area Description

The Okaba study site (coordinates: 7.40578°–7.41178°N, 7.79717°–7.80667°E) lies within the Enjema District of Ankpa Local Government Area, Kogi State, Nigeria. Geologically, the area resides within the Middle Benue Trough, a significant Cretaceous sedimentary basin[10,11]. The predominant local geology consists of sandstone, shale, siltstone, limestone, and clay sequences interbedded with coal seams belonging to the Mamu Formation[12]. Intensive coal seam extraction, combined with quarrying of ancillary minerals, has substantially altered the local landscape. Open-pit mining, overburden disposal, and spoil heap creation have accelerated geomorphic processes, resulting in severe deforestation, topsoil loss, gully erosion, and water quality degradation[13]. Figure 1

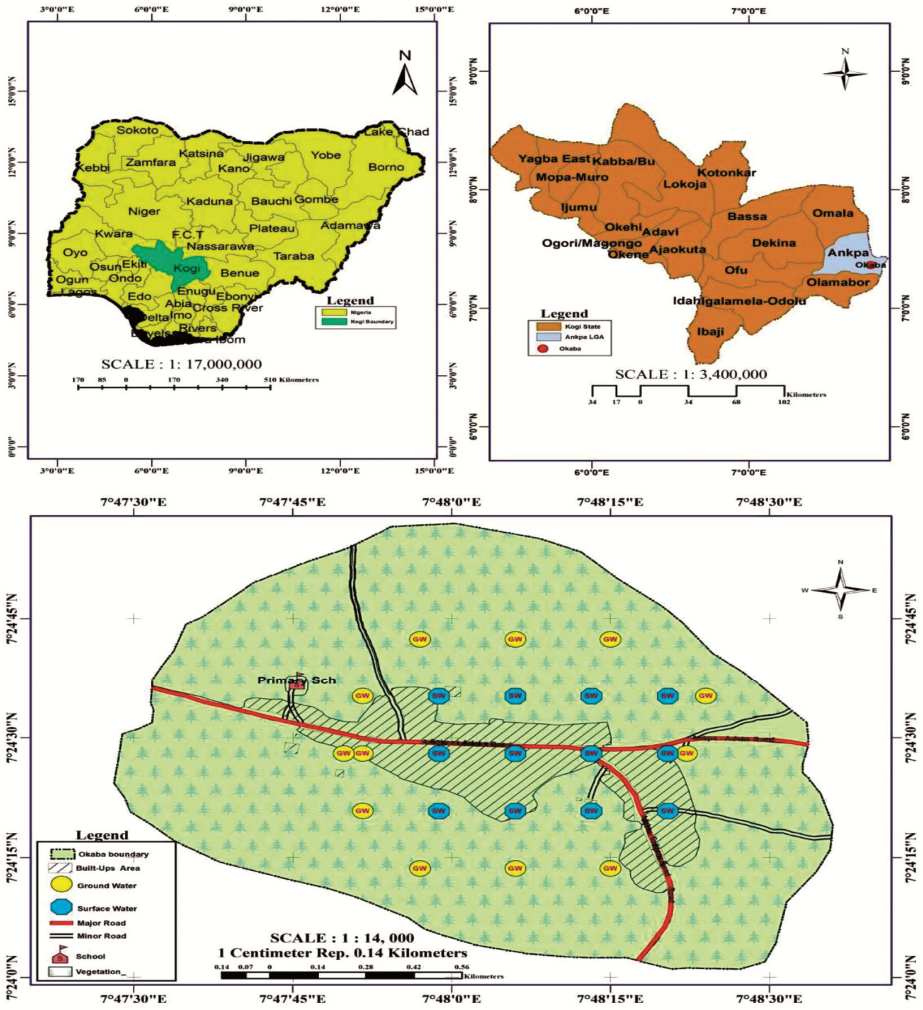


Fig. 1 — Map of Nigeria showing Kogi State, map of Kogi State showing Ankpa Local Government Area and the sampling location map of Okaba, Ankpa, Kogi. Base map created using QGIS (Version 3.34). Administrative boundaries obtained from GADM (Version 4.1) Boundary, Nigeria. Map layout prepared using Esri ArcGIS Pro

presents the map of Nigeria showing Kogi State, the map of Kogi State showing Ankpa Local Government Area, and the sampling location map of Okaba, Ankpa, Kogi[14-16].

2.2 Sample Collection Strategy

A stratified purposive sampling approach was implemented to obtain representative samples from all critical hydrological nodes within the study area. Field sampling occurred during the late rainy to early dry season transition (October–December 2024). Twenty-four water samples were collected from two major catchment systems affected by Okaba mining operations. Table 1 presents the geographical coordinates of water sampling locations in Okaba.

Surface water samples were obtained from streams and rivers at strategic positions: upstream (background) locations approximately 2–3 km above mining influence (SWA 1–3, SWA 13–15); midstream (proximal impact) points receiving direct drainage from active mine pits or coal washing facilities (SWA 4, SWA 16); and downstream (dispersal) locations 1–2 km below mining activities (SWA 5–7, SWA 17–19). Groundwater samples were collected from ten communal boreholes (SWA 8–12, SWA 20–24), selected based on proximity (within 5 km radius) to mining areas and their utilization as primary drinking water sources.

Strict contamination avoidance protocols[17] were followed during sample collection. Each 1-liter pre-cleaned polyethylene container and amber glass bottle was rinsed three times with source water before filling. For boreholes, water was pumped for a minimum of 5 minutes to purge the standing column before collection. In-situ parameters including pH, electrical conductivity (EC), total dissolved solids (TDS), and temperature were measured using a calibrated multiparameter probe (Hanna HI98194). For radionuclide analysis, amber glass bottle samples were immediately acidified to pH < 2 using ultrapure 6 M hydrochloric acid to prevent radionuclide adsorption onto container walls and inhibit microbial activity[17]. All samples were labeled, placed in coolers at 4 °C, and transported to the laboratory.

2.3 Sample Preparation and Gamma Spectrometry

Water samples for gamma spectrometry were prepared following protocols outlined in IAEA Technical Report Series No. 295[18]. Each sample was carefully evaporated at 80°C in pre-weighed Marinelli

Table 1 — Geographical Coordinates of Water Sampling Locations in Okaba

Sample ID	Latitude (°N)	Longitude (°E)	Source Type	Description/Proximity to Mining Activity
SWA1	7.40578	7.79967	Stream	Upstream, background control
SWA2	7.40578	7.80167	Stream	Upstream, background control
SWA3	7.40578	7.80367	Stream	Upstream, background control
SWA4	7.40778	7.79967	Stream	Midstream, receives direct mine drainage
SWA5	7.40778	7.80167	Stream	Downstream, community access point
SWA6	7.40778	7.80367	Stream	Downstream, community access point
SWA7	7.40978	7.79967	Stream	Downstream, community access point
SWA8	7.40978	7.80167	Groundwater	Community borehole within 2 km of mine
SWA9	7.40978	7.80367	Groundwater	Community borehole within 2 km of mine
SWA10	7.40578	7.80567	Groundwater	Community borehole within 2 km of mine
SWA11	7.40778	7.80567	Groundwater	Community borehole within 2 km of mine
SWA12	7.40978	7.80567	Groundwater	Community borehole within 2 km of mine
SWA13	7.40578	7.79767	River	Upstream tributary, background
SWA14	7.40778	7.79767	River	Upstream tributary, background
SWA15	7.40978	7.79767	River	Upstream tributary, background
SWA16	7.40378	7.80167	River	Midstream, adjacent to coal washing area
SWA17	7.41178	7.80167	River	Downstream, used for irrigation
SWA18	7.40778	7.79717	River	Downstream, used for irrigation
SWA19	7.40778	7.80617	River	Downstream, used for irrigation
SWA20	7.40378	7.79917	Groundwater	Borehole within 3-5 km of active pits
SWA21	7.40378	7.80417	Groundwater	Borehole within 3-5 km of active pits
SWA22	7.41178	7.79917	Groundwater	Borehole within 3-5 km of active pits
SWA23	7.41178	7.80417	Groundwater	Borehole within 3-5 km of active pits
SWA24	7.40978	7.80667	Groundwater	Borehole within 3-5 km of active pits

beakers to near-dryness, producing a stable residue. Beakers were sealed with airtight lids and stored for a minimum of 30 days to establish secular equilibrium between radium-226 (^{226}Ra) and its short-lived progeny (^{214}Pb, ^{214}Bi), and between thorium-232 (^{232}Th) and its progeny (^{228}Ac, ^{212}Pb, ^{208}Tl)[19,20].

Activity concentrations were determined using a p-type coaxial High-Purity Germanium (HPGe) detector (Canberra Industries, relative efficiency: 73.8 % at 1.33 MeV of ^{60}Co, energy resolution: 1.99 keV FWHM at 1332 keV). The detector was enclosed within a cylindrical shield comprising 5 cm low-background lead with inner linings of cadmium (1 mm) and copper (1 mm). Energy and efficiency calibration were performed using a certified mixed-radionuclide standard source traceable to the IAEA[21]. Quality assurance was maintained through procedural blank analysis, duplicate sample measurements, and certified reference material analysis (IAEA-447 and IAEA-448), following protocols described[22-23]. Minimum detectable activities (MDA) were calculated using Currie's method[24]: 0.05 Bq L^{-1} for ^{238}U, 0.03 Bq L^{-1} for ^{232}Th, and 0.10 Bq L^{-1} for ^{40}K. Spike recovery efficiencies ranged from 92% to 105%. Each prepared sample was counted for 86,400 seconds (24 hours)[25]. Spectral data acquisition and analysis were performed using Quantum Gold spectroscopy software (Version 2.0, Canberra)[26]. Background spectra were acquired periodically and background subtraction was applied to each sample spectrum.

Activity concentration Ac (Bq L^{-1}) for each radionuclide was calculated using the formula[27-29];

$$Ac = (C - B) / (\varepsilon \times I\gamma \times t \times V) \quad \text{... (1)}$$

where C = total counts under the photopeak, B = background counts, ε = detector efficiency, Iγ = emission probability, t = live counting time (seconds), and V = original water volume (L).

2.4 Radiological Hazard Indices

Several indices were computed from measured activity concentrations (C_U, C_{Th}, C_K for ^{238}U, ^{232}Th, and ^{40}K, respectively) to assess radiological safety;

Radium Equivalent Activity (Raeq): Weighted sum of activities for comparing gamma radiation output[30].

$$Ra_{eq}\ (Bq\ L^{-1}) = C_U + 1.43C_{Th} + 0.077C_K \quad \text{... (2)}$$

Gamma Radiation Index (Iγ): Screens gamma radiation hazard[30,31].

$$I\gamma = C_U/300 + C_{Th}/200 + C_K/3000 \quad \text{... (3)}$$

External Hazard Index (H_{ex}): Evaluates external gamma irradiation hazard[29,30].

$$H_{ex} = C_U/370 + C_{Th}/259 + C_K/4810 \quad \text{... (4)}$$

Outdoor Absorbed Dose Rate (D_{out}): Gamma dose rate in air at 1 m above ground[29,30].

$$D_{out}\ (nGy\ h^{-1}) = 0.462C_U + 0.604C_{Th} + 0.0417C_K \quad \text{... (5)}$$

Alpha Index (Iα): Screens excess alpha radiation exposure[32].

$$I\alpha = C_U / 200 \quad \text{... (6)}$$

Internal Hazard Index (H_{in}): Assesses internal exposure hazard[29,32].

$$H_{in} = C_U/185 + C_{Th}/259 + C_K/4810 \quad \text{... (7)}$$

Indoor Absorbed Dose Rate (D_{in}): Gamma dose rate inside a standard room[29,32].

$$D_{in}\ (nGy\ h^{-1}) = 0.92C_U + 1.1C_{Th} + 0.08C_K \quad \text{... (8)}$$

2.5 Ingestion Dose Assessment

Annual effective doses (AED) from radionuclide ingestion were calculated for three age groups (infants, children, adults) following UNSCEAR and WHO methodologies[3,33];

$$AED = Ac \times Iw \times Dc \quad \text{... (9)}$$

where Ac = activity concentration (Bq L^{-1}), Iw = annual water intake rate (L y^{-1}): 150 for infants, 350 for children, 500 for adults[3], and Dc = age-specific ingestion dose coefficient (μSv Bq^{-1}) from ICRP Publication 119[34]. Table 2 presents the age-specific ingestion dose coefficients.

Excess Lifetime Cancer Risk (ELCR) was estimated using;

$$ELCR = AED \times DL \times RF \quad \text{... (10)}$$

where AED is total annual effective dose (Sv y^{-1}), DL is average lifespan (70 years), and RF is fatal cancer risk factor (0.057 Sv^{-1}) as recommended by ICRP for public exposure[35].

2.6 Statistical Analysis

Statistical analyses were performed using IBM SPSS Statistics (Version 26). One-way Analysis of Variance (ANOVA) tested spatial variation in radionuclide concentrations across sampling

Table 2 — Age-Specific Ingestion Dose Coefficients (μSv Bq^{-1})

Radionuclide	Infants (1 yr)	Children (7-12 yrs)	Adults	Source
^{238}U	0.068	0.045	0.031	ICRP 119
^{232}Th	0.120	0.080	0.055	ICRP 119
^{40}K	0.021	0.014	0.0062	ICRP 119

locations. Post-hoc Tukey's Honestly Significant Difference (HSD) test identified specific location pairs with significant differences. Pearson correlation coefficients quantified relationships between radionuclide activities. Results are presented as mean ± standard deviation, with $p < 0.05$ considered statistically significant.

3 Results

3.1 Radionuclide Activity Concentrations

Measured activity concentrations of naturally occurring radionuclides in water samples from the Okaba mining region are summarized in Table 3, revealing substantial spatial variability.

Uranium-238 (^{238}U): Activity concentrations ranged from 44.24 ± 0.33 to 172.67 ± 2.39 Bq L^{-1}, with a mean of 104.80 Bq L^{-1}.

Thorium-232 (^{232}Th): Concentrations ranged from 21.66 ± 0.03 to 99.20 ± 0.91 Bq L^{-1}, with a mean of 51.49 Bq L^{-1}.

Table 3 — Activity Concentrations of Radionuclides in Water Samples from Okaba

Sample ID	CU (Bq L^{-1})	CTh (Bq L^{-1})	CK (Bq L^{-1})
SWA1	154.11 ± 2.11	61.01 ± 0.81	639.89 ± 4.01
SWA2	145.14 ± 2.09	68.09 ± 1.10	911.54 ± 5.66
SWA3	128.09 ± 1.90	59.11 ± 0.59	101.72 ± 0.18
SWA4	116.24 ± 1.54	44.34 ± 0.66	228.44 ± 1.16
SWA5	96.63 ± 0.94	22.43 ± 0.29	965.00 ± 4.89
SWA6	99.12 ± 1.21	26.21 ± 0.11	949.20 ± 4.23
SWA7	109.13 ± 1.01	28.26 ± 0.18	928.01 ± 4.14
SWA8	66.34 ± 0.71	44.11 ± 0.34	955.00 ± 4.46
SWA9	61.56 ± 0.15	45.76 ± 0.52	869.21 ± 3.77
SWA10	58.09 ± 0.52	41.56 ± 0.18	886.45 ± 3.06
SWA11	44.24 ± 0.33	43.66 ± 0.78	943.22 ± 4.64
SWA12	69.48 ± 0.79	47.07 ± 1.12	699.26 ± 2.98
SWA13	167.16 ± 2.07	99.20 ± 0.91	732.04 ± 2.91
SWA14	172.67 ± 2.39	59.32 ± 0.23	625.21 ± 2.31
SWA15	157.27 ± 2.01	84.13 ± 0.10	682.02 ± 2.11
SWA16	121.03 ± 1.88	58.14 ± 0.14	443.02 ± 1.98
SWA17	89.45 ± 0.12	36.12 ± 0.09	190.11 ± 0.89
SWA18	95.23 ± 0.86	44.24 ± 0.01	121.02 ± 0.06
SWA19	98.12 ± 0.93	41.06 ± 0.06	987.24 ± 4.32
SWA20	122.32 ± 1.63	21.66 ± 0.03	812.01 ± 3.53
SWA21	96.68 ± 0.97	60.24 ± 0.24	902.43 ± 4.24
SWA22	84.54 ± 0.72	89.77 ± 0.82	804.03 ± 3.92
SWA23	73.33 ± 0.64	48.01 ± 0.46	900.11 ± 4.23
SWA24	89.21 ± 0.61	62.22 ± 1.14	996.23 ± 4.08
Mean	104.80	51.49	719.64
Max	172.67 ± 2.39	99.20 ± 0.91	987.24 ± 4.32
Min	44.24 ± 0.33	21.66 ± 0.03	101.72 ± 0.18
Range	44.24–172.67	21.66–99.20	101.72–987.24

Potassium-40 (^{40}K): Displayed the highest absolute activities, ranging from 101.72 ± 0.18 to 987.24 ± 4.32 Bq L^{-1}, with a mean of 719.64 Bq L^{-1}.

Statistical Analysis: One-way ANOVA confirmed statistically significant spatial variation for all radionuclides ($p < 0.05$). Post-hoc Tukey HSD tests identified that upstream samples and proximal mining impact samples exhibited significantly higher activities than downstream and borehole samples ($p < 0.05$ for most comparisons). Pearson correlation analysis revealed moderate positive correlation between CU and CTh ($r = 0.61$, $p < 0.001$), supporting common origin. Weak correlations were observed between CU and CK ($r = 0.32$, $p = 0.052$) and CTh and CK ($r = 0.18$, $p = 0.283$).

3.2 Radiological Hazard Indices

Calculated radiological hazard parameters are presented in Table 4. All indices showed statistically significant variation across samples ($p < 0.05$). Table 5 summarizes the radiological hazard indices compared with safety limits.

Radium Equivalent Activity (Raeq): Values ranged from 341.69 to 884.73 Bq L^{-1} (mean: 573.87 Bq L^{-1}). Notably, 87.5 % of samples exceeded the recommended safety limit.

Absorbed Dose Rates: Mean outdoor (Dout) and indoor (Din) absorbed dose rates were 109.53 nGy h^{-1} and 210.63 nGy h^{-1}, respectively—1.86 and 2.51 times higher than world average values (59 and 84 nGy h^{-1}) reported by UNSCEAR[33].

Hazard Indices: External (Hex) and internal (Hin) hazard indices ranged from 0.42–0.99 (mean: 0.63) and 0.60–1.44 (mean: 0.91), respectively. While mean Hex remained below unity, mean Hin approached it, and 29.2 % of samples exceeded Hin > 1.

3.3 Annual Effective Dose and Excess Lifetime Cancer Risk from Ingestion

Annual effective doses from water ingestion were calculated for infants, children, and adults. Table 6 presents the annual effective doses by age group compared with WHO limit.

Radionuclide Contribution: Across all demographics, ^{232}Th was the predominant contributor to total ingestion dose, accounting for approximately 87–90 % of mean dose. Uranium-238 contributed approximately 10–12 %, while ^{40}K contributed less than 1 %. Table 7 presents the excess lifetime cancer risk by age group.

All values substantially exceed the internationally accepted benchmark risk level of 1.0×10^{-3}. For

Table 4 — Radiation Hazard Indices for Water Samples from Okaba

Sample ID	Raeq (Bq L^{-1})	Iγ	Hex	Dout (nGy h^{-1})	Iα	Hin	Din (nGy h^{-1})
SWA1	884.73	1.032	0.785	134.73	0.771	1.202	260.08
SWA2	617.76	1.128	0.845	146.19	0.726	1.237	281.35
SWA3	510.32	0.756	0.596	99.10	0.640	0.942	191.00
SWA4	496.09	0.685	0.533	98.43	0.581	0.847	173.99
SWA5	437.17	0.756	0.547	101.21	0.483	0.810	190.77
SWA6	341.69	0.778	0.566	106.19	0.496	0.834	195.96
SWA7	345.87	0.814	0.597	97.12	0.546	0.892	205.73
SWA8	700.69	0.760	0.548	92.33	0.332	0.727	185.95
SWA9	794.37	0.724	0.524	88.91	0.308	0.690	176.51
SWA10	615.15	0.698	0.508	86.14	0.290	0.659	170.08
SWA11	635.05	0.680	0.484	89.69	0.221	0.604	164.18
SWA12	720.08	0.700	0.515	167.67	0.347	0.703	171.64
SWA13	517.38	1.297	0.987	141.67	0.836	1.439	321.47
SWA14	498.05	1.081	0.826	151.91	0.863	1.292	274.13
SWA15	523.76	1.172	0.892	109.51	0.786	1.317	291.79
SWA16	483.19	0.842	0.644	75.76	0.605	0.971	210.74
SWA17	429.59	0.542	0.421	111.30	0.447	0.662	137.24
SWA18	427.88	0.579	0.453	103.46	0.479	0.711	145.96
SWA19	393.64	0.861	0.629	118.68	0.491	0.894	214.42
SWA20	557.49	0.787	0.583	126.81	0.612	0.745	201.32
SWA21	767.63	0.924	0.681	100.41	0.483	0.943	227.40
SWA22	642.72	0.999	0.742	120.34	0.423	0.971	240.85
SWA23	801.48	0.785	0.601	90.10	0.367	0.769	192.28
SWA24	631.21	0.940	0.688	71.07	0.446	0.930	230.21
Mean	573.87	0.847	0.633	109.53	0.524	0.908	210.63
Max	884.73	1.297	0.987	167.67	0.863	1.439	321.47
Min	341.69	0.542	0.421	71.07	0.221	0.604	137.24

Table 5 — Summary of Radiological Hazard Indices Compared with Safety Limits

Parameter	Mean ± SD	Range	Safety Limit	% Exceeding Limit	Fold Exceedance
Raeq (Bq L^{-1})	573.87 ± 154.32	341.69–884.73	370 Bq kg^{-1}*	87.5% (21/24)	1.55×
Iγ	0.847 ± 0.193	0.542–1.297	1	12.5% (3/24)	—
Hex	0.633 ± 0.151	0.421–0.987	1	0%	—
Dout (nGy h^{-1})	109.53 ± 24.81	71.07–167.67	59	100%	1.86×
Iα	0.524 ± 0.184	0.221–0.863	1	0%	—
Hin	0.908 ± 0.231	0.604–1.439	1	29.2% (7/24)	—
Din (nGy h^{-1})	210.63 ± 49.15	137.24–321.47	84	100%	2.51×

*Raeq limit is presented for comparative purposes only, as the limit is originally specified for building materials (Bq kg^{-1}).

Table 6 — Annual Effective Doses by Age Group Compared with WHO Limit

Age Group	Mean AED ± SD (mSv y^{-1})	Range (mSv y^{-1})	WHO Limit (mSv y^{-1})	Fold Exceedance	% Exceeding Limit
Infants	6.88 ± 2.72	3.37–13.06	0.1	68.8×	100%
Children	4.59 ± 1.81	2.24–8.70	0.1	45.9×	100%
Adults	3.15 ± 1.25	1.54–5.98	0.1	31.5×	100%

infants at the highest exposure point (SWA13, AED = 13.06 mSv y^{-1}), ELCR reaches approximately 52.1 × 10^{-3} (1 in 19).

4 Discussion

Environmental radioactivity enhanced by anthropogenic activities such as mining presents substantial challenges to ecological integrity and public health. The Okaba coalfield, characterized by intensive and largely unregulated artisanal mining, exemplifies a high-risk environment where natural geochemical equilibrium has been disrupted.

4.1 Comparison with International Studies

Table 8 presents a comparison of mean radionuclide concentrations and dose rates with other

Table 7 — Excess Lifetime Cancer Risk by Age Group

Age Group	Mean AED (Sv y^{-1})	ELCR ($\times 10^{-3}$)	Range ($\times 10^{-3}$)	Benchmark	% Exceeding Benchmark
Infants	6.88×10^{-3}	27.45	13.45–52.10	1.0×10^{-3}	100%
Children	4.59×10^{-3}	18.31	8.94–34.70	1.0×10^{-3}	100%
Adults	3.15×10^{-3}	12.57	6.14–23.85	1.0×10^{-3}	100%

Table 8 — Comparison of Mean Radionuclide Concentrations and Dose Rates with Other Studies

Location	^{238}U (Bq L^{-1})	^{232}Th (Bq L^{-1})	^{40}K (Bq L^{-1})	D out (nGy h^{-1})
Okaba, Nigeria	104.80	51.49	719.64	109.53
Enugu, Nigeria	128.50	—	—	—
Other Nigerian coalfields	67.40	—	—	—
East Bokaro, India	45.2	32.8	486.5	—
Nile River, Egypt	0.62	0.18	2.53	—
Punjab, Pakistan	48.50	42.80	612.50	—
Makoko, Nigeria	—	—	—	85.2
World Average	—	—	—	59

studies. Mean uranium concentration (104.80 Bq L^{-1}) exceeds values reported in other Nigerian coalfield waters (67.40 Bq L^{-1})[36], though remaining below extreme levels found in Enugu fields (128.50 Bq L^{-1})[37]. Mean thorium concentration (51.49 Bq L^{-1}) aligns with regional backgrounds[38]. The notably high ^{40}K activity (mean: 719.64 Bq L^{-1}) represents the most significant contributor to overall gamma radioactivity.

4.2 Radiological Hazard Implications

Derived radiological hazard indices provide direct risk characterization. Absorbed dose rates (D_{out}: 109.53 nGy h^{-1}; D_{in}: 210.63 nGy h^{-1}) and Radium Equivalent activity (mean Ra_{eq}: 573.87 Bq L^{-1}) are significantly elevated above global averages. Primary mechanisms likely include: (i) geochemical mobilization through acid mine drainage creating acidic conditions that increase uranium and radium solubility; and (ii) physical mobilization through erosion and surface runoff transporting fine, radioelement-enriched particulates from mine pits and waste dumps.

Calculated annual effective doses from ingestion substantiate public health concerns. Mean doses for all age groups are orders of magnitude higher than those reported from studies in India (0.02–0.08 mSv y^{-1})[39], Egypt (0.01–0.03 mSv y^{-1})[40], Pakistan (0.05–0.12 mSv y^{-1})[41], and other Nigerian coal areas (0.15–0.48 mSv y^{-1})[36,37]. Absorbed dose rates and Ra_{eq} values are also consistently higher than values reported from other Nigerian regions[42]. All surpass WHO recommended reference dose level of 0.1 mSv y^{-1} for drinking water by factors of 31.5–68.8[3]. Disproportionate infant burden is physiologically rational: higher metabolic rates, greater intestinal absorption efficiency, and lower body mass result in higher committed doses per unit intake.

Consequent Excess Lifetime Cancer Risk, particularly for infants at high-exposure locations (up to 52.1×10^{-3}), transitions findings from an environmental study to a pressing public health warning and indicates inconsistency with international safety standards[43].

4.3 Spatial Analysis and Contamination Source Identification

Spatial radionuclide distribution clearly implicates mining activities as dominant source, with hydrological pathways governing dispersal. Primary Source – Mining Waste and Excavated Material: Disturbance of coal seams and overburden represents principal mechanism releasing NORMs. This is supported by moderate positive correlation ($r = 0.61$) between ^{238}U and ^{232}Th, indicating common lithogenic origin.

Natural Background Enhancement: Elevated concentrations in upstream surface samples SWA13–SWA15 suggest natural geological enrichment from uranium-bearing organic-rich shales and sandstones of the Mamu Formation, which are known to contain elevated uranium concentrations due to organic matter content[10,12].

Point Source Contamination: Highest recorded concentrations are typically associated with direct point sources including active mine drainage channels, coal washing effluent discharge points, and surface runoff from uncovered spoil heaps.

Groundwater Contamination: Detection of elevated uranium and radium in borehole water confirms non-

point source pathway into groundwater aquifers via infiltration of contaminated surface water and AMD.

4.4 Ecological Risk Assessment

The elevated concentrations of radionuclides measured in Okaba's water bodies necessitate consideration of potential impacts on the local aquatic ecosystem. The measured concentrations of ^{238}U (mean: 104.80 Bq L^{-1}) and ^{232}Th (mean: 51.49 Bq L^{-1}) are significantly above typical freshwater background levels (generally <0.1 Bq L^{-1}). Uranium is of particular ecological concern due to its combined radiotoxic and chemotoxic properties, with known bioaccumulation potential in aquatic organisms[42,44].

4.5 Regulatory Benchmarking and Policy Implications

Systematic Exceedance of International Limits: Data consistently violates key international safety standards;

i Mean Radium Equivalent Activity (573.87 Bq L^{-1}) surpasses 370 Bq kg^{-1} safety limit[30]

ii Calculated Annual Effective Doses drastically exceed WHO recommended limit[3]

iii Resulting Excess Lifetime Cancer Risk exceeds commonly accepted benchmark by factor of 12.6

Critical Gap in National Regulation: Paramount finding is absence of specific, enforceable national standards in Nigeria for radionuclide content in drinking water or mining effluent. This regulatory vacuum fails to protect populations in mining regions and is inconsistent with international safety standards[43].

5 Conclusion

This comprehensive radiological assessment of water resources in the Okaba coal mining area demonstrates that intensive mining operations have significantly exacerbated natural background radioactivity, resulting in substantial contamination of both surface and groundwater. The activity concentrations of ^{238}U, ^{232}Th, and ^{40}K, along with calculated hazard indices, exceed global averages and relevant safety benchmarks in numerous sample locations. Specifically, 100 % of samples exceeded global average dose rates, 87.5% exceeded the Raeq safety limit, and 29.2 % exceeded the Hin safety limit.

The study identifies a clear radiological health threat, driven primarily by ingestion of thorium and uranium series radionuclides. Infants are the most critically vulnerable demographic, facing annual effective doses (mean: 6.88 mSv y^{-1}) exceeding WHO guidelines by factor of 69 and associated cancer risks (ELCR: 27.45×10^{-3}) mandating immediate intervention. Contamination is spatially heterogeneous, pinpointing specific high-impact zones proximate to mining activities and certain geological formations.

Therefore, the situation in Okaba transcends academic interest; it represents tangible environmental justice and public health issues where community reliance on contaminated water poses demonstrable long-term risk. Sustainable mining and community health are inextricably linked; this study provides empirical evidence necessary to drive change.

References

1 United Nations Scientific Committee on the Effects of Atomic Radiation, *Sources and Effects of Ionizing Radiation UNSCEAR 2000 Report to the General Assembly*, United Nations, New York, 2000.

2 International Atomic Energy Agency, *Radiation Protection and Safety International Basic Safety Standards*, IAEA Safety Standards Series No GSR Part 3, IAEA, Vienna, 2018.

3 World Health Organization, *Guidelines for Drinking-Water Quality*, 4th ed., Incorporating the First Addendum, WHO, Geneva, 2017.

4 Salih N F, *Arab J Geosci*, 15 (2022) 1157.

5 Mbogu N E & Inoni O E, *J Min Geol*, 54 (2018) 123.

6 Ademola J A, Bello A K & Adejumobi A C, *J Radiat Res Appl Sci*, 7 (2014) 249.

7 Farai I P & Jibiri N N, *Radiat Prot Dosim*, 88 (2000) 247.

8 Jibiri N N, Farai I P & Alausa S K, *Radiat Environ Biophys*, 50 (2011) 67.

9 Ibrahim M A, Yusuf M O & Mohammed S I, *J Appl Sci Environ Manage*, 24 (2020) 659.

10 Benkhelil J, *J Afr Earth Sci*, 8 (1989) 251.

11 Obaje N G, *Geology and Mineral Resources of Nigeria*, *Springer*, *Berlin*, 2009.

12 Ezeigbo H I & Ozoko D C, *Niger J Min Geol*, 23 (1987) 45.

13 Adeniji A O, Okoh O O & Okoh A I, *Arch Environ Contam Toxicol*, 76 (2019) 657.

14 International Atomic Energy Agency, *Analytical Quality Control for Radioactivity Measurement*, IAEA-TECDOC-1401, IAEA, Vienna, 2024.

15 International Atomic Energy Agency, *Measurement of Radionuclides in Food and the Environment*, Technical Report Series No. 295, IAEA, Vienna, 1989.

16 Tchokossa P, Olomo J B & Osibote O A, *Nucl Instrum Methods Phys Res Sect A*, 353 (1994) 553.

17 Tsivou M, Nikolopoulos K G, Chrysochou E, Pappa E, Pashalidis A & Papastefanou C T, *J Environ Radioact*, 101 (2010) 507.

18 Darwish D A E *et al*., *J Radiat Res Appl Sci*, 8 (2015) 17.

19 Salih N F, *ARO-Sci J Koya Univ*, 6 (2018) 1.

20 Khandaker M U, *Appl Radiat Isot*, 69 (2011) 885.

21 Currie L A, *Anal Chem*, 40 (1968) 586.

22 Khandaker M U, Wahib N B M, Amin Y M, Kassim H A & Bradley D A, *Radiat Phys Chem*, 88 (2013) 1.

23 Canberra Industries, *Quantum Gold Spectroscopy Software*, v2.0, Canberra Industries, 2016.
24 Fasae K P & Isinkaye M O, *J Radiat Res Appl Sci*, 11 (2018) 317.
25 Nisar A, Mohammed S A, Mohamad S J & Norlaili A K, *J Environ Sci Health Part A*, 53 (2018) 1.
26 Salih N F, *Management of Natural Radioactivity in Drinking Water*, *Springer, Cham*, 2022.
27 Angeleska A *et al*., *IOSR J Pharm*, 7 (2017) 20.
28 Alias M *et al*., *Malays J Anal Sci*, 12 (2008) 195.
29 Salih N F, *Isot Environ Health*, 55 (2018) 80.
30 United Nations Scientific Committee on the Effects of Atomic Radiation, *Sources, Effects and Risks of Ionizing Radiation — 2020/2021 Report to the General Assembly with Scientific Annexes*, UNSCEAR, 2021.
31 International Commission on Radiological Protection, *ICRP Publication 119*, Annals of the ICRP, 41 (1S) 2012.
32 International Commission on Radiological Protection, *ICRP Publication 103*, Annals of the ICRP, 37 (2) 2007.
33 United Nations Scientific Committee on the Effects of Atomic Radiation, *Sources and Effects of Ionizing Radiation: UNSCEAR 2008 Report*, United Nations, New York, 2008.
34 Adegunwa A O, Awojide S H & Ore O T, *Nucl Sci*, 4 (4) (2019) 66.
35 Owoade L, Alakiu H, Akinde K & Nwankwo C U, *Health Phys*, 117 (5) (2019) 504.
36 Mahato M K, Singh P K, Tiwari A K & Singh A K, *Expo Health*, 8 (4) (2016) 265.
37 El-Gamal H, Sefelnasr A & Salaheldin G, *Water*, 11 (2) (2019) 311.
38 Kolo M T *et al*., *PLOS ONE*, 2016.
39 Jibiri N N, Ugbechie A, Sowunmi A A & Akomolafe I R, *Mar Pollut Bull*, 192 (2023) 114992.
40 Rahman S U, Mehdi S A, Jahanzeb Q, Rafique M, Tareen A D K, Iqbal J, Talat Iqbal & Jabbar A, *J Radiat Nucl Appl*, 3(1) (2018) 23.
41 International Atomic Energy Agency, *Radiation Protection and Safety of Radiation Sources: International Basic Safety Standards*, General Safety Requirements Part 3, IAEA, 2014.
42 International Commission on Radiological Protection, *ICRP Publication 108*, Annals of the ICRP, 38(4-6), 2008.
43 Esri, *ArcGIS Pro (Version 3.5)* (Computer software), Environmental Systems Research Institute, Redlands, CA, 2025.
44 QGIS Development Team, *QGIS Geographic Information System (Version 3.34)* (Computer software), Open Source Geospatial Foundation, 2024.
45 Hijmans R J, *Boundary, Nigeria, 2015*, University of California, Berkeley, 2015.